

SPACE CHARGE DYNAMICS SIMULATED IN 3-D IN THE CODE ORBIT *

A.U.Luccio, N.L. D'Imperio, J. Beebe-Wang
Brokhaven National Laboratory, Upton, NY, USA

Abstract

Several improvements have been done on space charge calculations in the PIC code ORBIT[1], specialized for high intensity circular hadron accelerators. We present results of different Poisson solvers in the presence of conductive walls.

1 PIC TRACKING WITH SPACE CHARGE

ORBIT uses a split operator technique. PIC particles[2] are propagated in the bare lattice using maps generated by MAD[3]. Then, space charge transverse momentum kicks and longitudinal energy kicks are applied.

2 DIFFERENTIAL POISSON SOLVERS

To find the scalar electric Φ and the magnetic vector potential \vec{A} , the herd is binned on a grid according to $(x, y, c\Delta t)$ to find the charge density ρ , and according to $(p_x, p_y, \Delta p/p)$, to find the current density \vec{j} . Then, we solve the partial elliptic differential equations (Poisson's) for $Q \rightarrow P$

$$\nabla^2 \Phi(P) = -\frac{\rho(Q)}{\epsilon_0} \quad ; \quad \nabla^2 \vec{A}(P) = -\frac{\vec{j}(Q)}{\mu_0} \quad (1)$$

In *ORBIT* we implemented two differential 2D solvers (i) LU Decomposition plus matrix multiplication, and (ii) Successive Over Relaxation (SOR).

For (i), express the Laplacian operator ∇^2 in discrete form on a $M \times N$ grid that extends to wall. For the first of Eqs.(1) it is (the second is formally identical):

$$-4\pi\rho_{ij} = \mathcal{L}_{ij}^{kl}\Phi_{kl} \quad ; \quad \Phi(P) = -\frac{1}{4\pi}\mathcal{L}^{-1}\rho(Q) \quad (2)$$

- this is an $M^2 \times N^2$ band-sparse matrix (δ is Kronecker's), whose inverse is unfortunately not sparse (Fig.1) -

$$\mathcal{L}_{ij}^{kl} = -4\delta_i^k\delta_j^l + \delta_{i+1}^k\delta_j^l + \delta_{i-1}^k\delta_j^l + \delta_i^k\delta_{j+1}^l + \delta_i^k\delta_{j-1}^l$$

and multiply the inverse by the $(M \times N)$ $\vec{\rho}$

For (ii), solve by iteration, starting with a guess. At step $k + 1$ the discretized Poisson's is

$$\Phi_{i,j}^{k+1} = \frac{1}{4} (\Phi_{i-1,j}^k + \Phi_{i,j+1}^k + \Phi_{i+1,j}^k + \Phi_{i,j-1}^k - \rho_{i,j}) .$$

Since the beam density evolves slowly from one space charge node to the next, iterative techniques show rapid convergence.

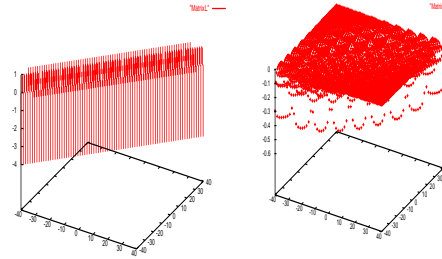


Figure 1: Direct and inverse Laplace Matrix.

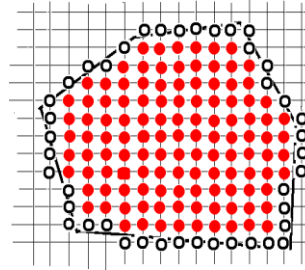


Figure 2: Solving with perfectly conducting walls

Better iterative procedures used were: Basic SOR (most efficient for small grids, $M, N < 128$), SOR with Chebyshev acceleration (large grid), and Conjugate Gradient, that showed the most rapid convergence.

Fig.2 schematically shows how to achieve a solution of the system of Eq.(2). Walls are represented by n empty dots. the interior by m full dots. The system of equations is exactly determined: $n + m$ known quantities, i.e. $\Phi = 0$ at the n empty dots and ρ at the m full dots; $m + n$ unknowns, i.e. m values of Φ to be calculated at the full dots and ρ_{image} at the n empty dots.

3 3-D TREATMENT OF SPACE CHARGE

Basic ideas:

- Space is the independent variable;
- To solve Poisson with all particles at the same time, at each space charge node in the lattice we expand the beam (Fig.3);
- 3.rd dimension is obtained by slicing the beam (Fig.4)

We use a transverse grid terminated at wall boundary, and a longitudinal grid that covers the length of the beam bunch. For long bunches in synchrotrons it is reasonable to make longitudinal grid steps much larger than in the transverse dimension. This is justified since (i) the space charge

* work supported by the US Department of Energy

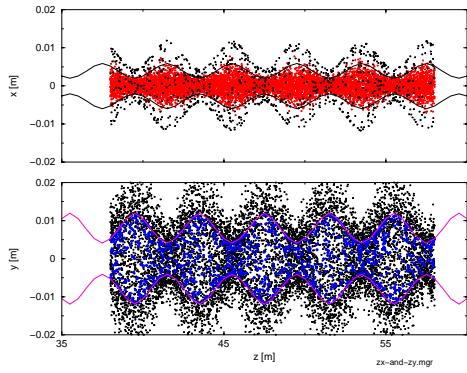


Figure 3: Expanded matched beam. Beam envelope is also shown

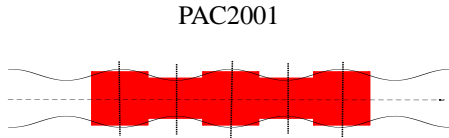


Figure 4: Slicing a beam. Wavy lines: envelope of the beam (β -wave). Dashed vertical lines: planes where to solve Poisson

distribution varies smoothly along the beam, and (ii) the motion along the beam is much slower than in the transverse.

We cut the beam in slices, long enough that the average density, the transverse aspect ratio of the slice, and the wall configuration around the slice can be considered constant.

$$\rho(x, y, z) = \rho_{\perp}(x, y) \rho_{\parallel}(z).$$

and only solve the 2D transverse problem simultaneously in each slice by parallel computation. A slice length is a fraction of the distance between successive envelope waists and is associated with the local wall configuration, stored together with the the transfer maps to completely characterize the machine. A similar approach is been used by L.G.Vorobiev *et al* at Michigan [4] [5].

4 COMPARISON OF 2-D SOLVERS

We compared the SC field calculated with integral solvers (BF and FFT, of a previous version of ORBIT) with a SOR differential solver on a 256×256 grid, conductive walls, and a Gaussian random beam in the chamber center (Fig.5).

The BF field goes to zero at large distance, while SOR ends at the walls with a finite value, where the image charge density is equal to the field and the field lines are perpendicular. The sum of the image charges equals the total of the real charges. In this case the images are uniformly distributed.

Another example: potential and image on the walls calculated with for a Gaussian distributed beam off center in the chamber (Fig.6).

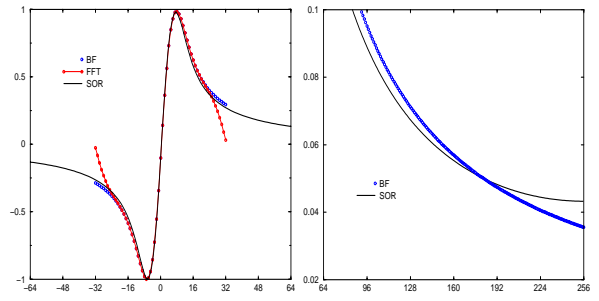


Figure 5: Comparison of field between 2-D BF and SOR

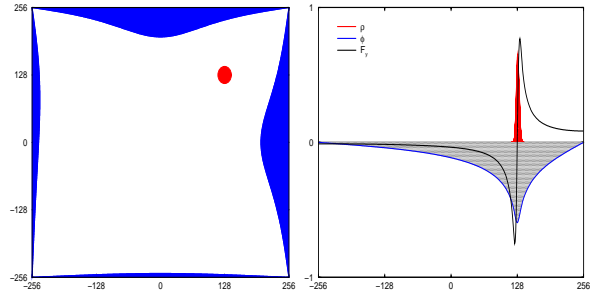


Figure 6: Beam offset in x and y in a square chamber. (a) real charge and image charge, (b) ρ , Φ , and E

5 3-D FORCES IN A LONG BEAM

Transverse kicks depend on the transverse aspect ratio of a slice (Fig.7). For the same φ , the force is on the average larger where the value of the Twiss β function is smaller, and vice-versa. This is shown in Fig.7 and Fig.8 from a SOR simulation of a FODO lattice.

Once we have Φ , the space charge force and the momentum kick on each macro are

$$\vec{F}(P) = \frac{e}{\gamma^2} \vec{\nabla} \phi \quad ; \quad \frac{\Delta \vec{p}}{p} = \frac{1}{p} \int \vec{F} dt. \quad (3)$$

With $dt = \Delta t = L/\beta c$, the transverse momentum kick and the longitudinal energy kick are

$$\frac{\delta p_{\perp}}{p} = \varphi \frac{\partial \phi}{\partial r} L_{\perp} \quad ; \quad \frac{\delta \Delta E}{E} = \beta^2 \varphi \frac{\partial \phi}{\partial z} L_{\parallel} \quad (4)$$

with the separation between successive transverse SC kicks L_{\perp} , the separation between longitudinal kicks L_{\parallel} ,

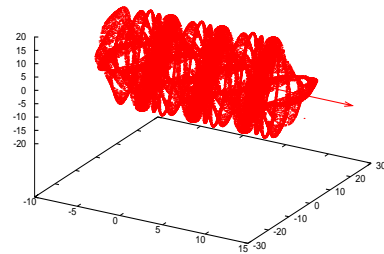


Figure 7: Sliced expanded beam in 3D. The aspect ratios of different slices are evident

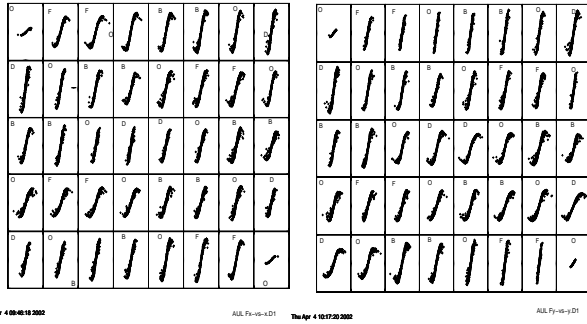


Figure 8: (a) SC force F_x vs. x in each of a 40-slice beam whose central slice is in a defocusing lattice location, (b) SC force F_y vs. y

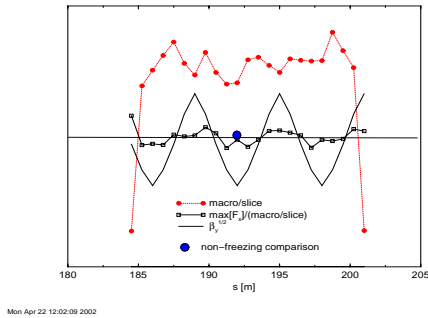


Figure 9: Maximum transverse kick in a 9-slice beam (AGS) compared with 2D calculation

the perveance

$$\wp = \frac{4\pi\lambda qhr_0}{\Delta x\beta^2\gamma^3 m_0},$$

with λ the charge per unit length and Δx the size of a square grid cell.

Transverse kicks depend on the transverse aspect ratio of a slice. For the same \wp , the force is on the average larger where the value of the Twiss β function is smaller, and vice-versa (Fig.9).

A longitudinal kick calculated from the difference of potential between analogous (x, y) points in the median transverse plane of successive slices (Fig.10) is compared with the traditional formula for a beam of radius a in a round pipe of radius b [6].

$$(\Delta E)_{SC} \propto Z_0 \frac{\lambda'}{2\gamma^2} \left[1 + 2 \ln \frac{b}{a} + f(r) \right] \quad (5)$$

Z_0 is the impedance of free space and ' λ' ' the charge gradient along the beam.

Fig.11 is a 3D rendition of the longitudinal force vs. x in the horizontal plane $y = 0$.

6 REFERENCES

[1] J.D.GALAMBOS, J.A.HOLMES, D.K.OLSEN A.LUCCIO and J.BEEBE-WANG: *Orbit User's Manual Vers. 1.10*. Technical Report SNS/ORNL/AP 011, Rev.1, 1999.

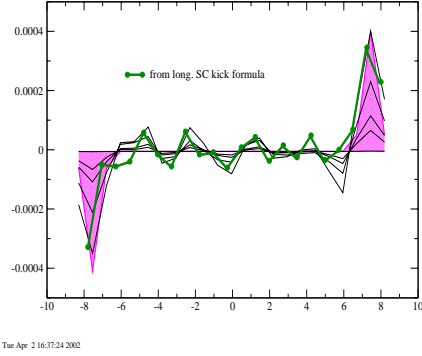


Figure 10: Longitudinal SC energy kick in a 9-slice beam (AGS). Each line: distribution of kick for various x, y . Thick line: simulation that uses the standard equation

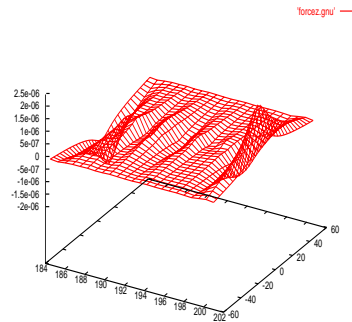


Figure 11: Longitudinal energy kick in 3D

[2] R.W.HOCKNEY and J.W.EASTWOOD: *Computer Simulation Using Particles*. Adam Hilger, IOP Publishing, New York, 1988.

[3] H.GROTE and F.CH.ISELIN: *The MAD program, Vers.8.19*. Technical Report CERN/SL/90-13, Geneva, Switzerland, 1996.

[4] L.G.VOROBIEV and R.C.YORK: *Beam Dynamics Modeling By Sub-Three-Dimensional Particle-In-Cell Code*. In: *Proc. Particle Accelerator Conference 2001*, 2001. Paper RPAAH097.

[5] L.G.VOROBIEV and R.C.YORK: *Method Of Template Potentials To Find Space Charge Forces For High-Current Beam Dynamics Simulation*. In: *Proc. Particle Accelerator Conference 2001*, 2001. Paper RPAAH098.

[6] A.W.CHAO: *Physics of Collective Beam Instabilities in High Energy Accelerators*. Wiley, New York, 1993.